Journal of Sound and Vibration (1998) **214**(1), 1–15

A COMPARISON OF MODAL EXPANSION AND TRAVELLING WAVE METHODS FOR PREDICTING ENERGY FLOW IN BEAM STRUCTURES

JIE PAN

Department of Mechanical and Materials Engineering, The University of Western Australia, WA 6907, *Australia*

AND

JIAQIANG PAN

Department of Mechanical Engineering, Zhejiang University, Hangzhou 310027, *P.R. China*

(*Received* 27 *November* 1996, *and in final form* 25 *November* 1997)

Both modal expansion and travelling wave methods are commonly used for predicting the response and vibrational energy flow in structures. They describe the same structural wave motion problem from different viewpoints. In this paper, energy flows carried by the torsional and flexural waves in beam structures are predicted by these two methods and the results are compared. It is shown that the convergence property of the energy flow predicted by the modal expansion method may be poor in the vicinity of the forcing location. The limitation of using a finite number of continuous mode shape functions to represent the discontinuity at the forcing location is illustrated. It is observed that the energy flow predicted by the modal expansion method oscillates about the exact energy flow obtained by the travelling wave method. The sources of the fluctuation are investigated. The study also suggests that spatial averaging of the oscillated energy flow may give a better approximation of the exact energy flow without using an extremely large number of modes.

1. INTRODUCTION

The dynamic response of an elastic structure can be described either by the modal expansion method (MEM) or the travelling wave method (TWM). The former method is based on the eigensolutions of the structural wave equation with homogeneous boundary conditions. According to the modal expansion theory [1], the structural response to any forcing function can be described as the superposition of all the eigenmodes. The latter method employs travelling wave components in all possible directions of the structure and the structural response is due to the superposition of the travelling wave components. For flexural waves in a beam, extra non-propagating wave solutions have to be included to satisfy the conditions of displacement continuity and force equilibrium at the boundaries, coupling joints and forcing locations. It is well known that the resonance response predicted by the modal expansion method can be interpreted as the coincidence superposition of travelling waves with opposite wave-number vectors described as incident and reflected waves.

Because the two methods describe the same wave motion, they are expected to be interchangeable. Although both modal expansion and travelling wave methods can be used for the prediction of energy flow in structures, there are cases where the modal expressions

0022–460X/98/260001 + 15 $25.00/0/sv971465

of the energy flow and structural response are more convenient and computationally efficient. Examples are band-limited energy flow, energies [2, 3] and the structural response to the excitation of PZT actuators [4]. However, the equivalence of the two methods in theoretical development does not guarantee the equivalent numerical properties when used in the calculation of energy flow in a structure. Because the response of the structure cannot be practically represented by an infinite number of eigenmodes, convergence in its calculation using the modal approach should be questioned, particularly in the near field of the driving force. Even though a good convergence is obtained for a given number of modes used for the prediction of the structure response, the same number of modes may not satisfy the convergence requirements for the derivatives of the response. When energy flow in the structure is calculated, the higher order derivatives of the displacement response are required to calculate the tensile force, shear force and rotating moments in the structure. As the convergence property of the higher order derivatives is usually poorer than that of the displacement response, the accuracy in the prediction of the energy flow can be limited [2]. For the study of the active control of structural vibrations, the design of the physical system involves the analysis of the structual/actuator interactions. An accurate description of the structural response near the actuator and sensor locations is important for estimating the control system behaviour. The convergence problem in the model prediction of the physical systems may affect the robustness of feedback control systems [5].

The objective of this paper is to study the effect of truncation error of the MEM on the prediction of structural energy flow. The significance of this subject has been emphasized by many authors [6]. Although it is well known that the accuracy of modal approach in the prediction of system response is related to the number of modes taken into account and that the accuracy diminishes at the near-field of sources and certain boundary types, little work has been done on this truncation effect on the higher order derivatives of the response. Any error in the prediction of higher order derivatives of the response will directly affect the prediction accuracy of energy flow in the system. Furthermore, the study of the characteristics of the modal truncation may provide a post-processing method to reduce the induced error without using an extremely large number of modes.

In this paper the energy flow carried by the torsional and flexural waves in a thin beam is calculated using both MEM and TWM. The results are compared and used to illustrate the convergence properties associated with the modal expansion approach.

2. TORSIONAL VIBRATION OF A THIN ROD

In the first example, the torsional response of a thin rod to a harmonic torque $M_0 e^{j\omega t}$ at $x = x_0$ is considered. Although the solution of the torsional response by either the modal expansion method or travelling wave method is well known, the comparison of the energy flow calculated by the two methods may improve our understanding of the convergence properties in the prediction of torsional energy flow.

2.1. FORCED RESPONSE FROM MEM AND TWM

The torsional equation of motion of a thin rod with a harmonic torque acting at $x = x_0$ can be written as:

$$\frac{\partial^2 \tilde{\theta}}{\partial x^2} - \frac{1}{c_T^2}\frac{\partial^2 \tilde{\theta}}{\partial t^2} = \frac{M_0 e^{j\omega t}}{GI_T}\delta(x - x_0) \tag{1}$$

where $\tilde{\theta}(x, t)$ is the angular displacement of the cross section at x. $G = G_0(1 + j\eta_T)$ is the complex shear modulus and η_T is the shear loss factor. I_T is the moment of the cross section around the rod axis. $c_T = \sqrt{G/\rho}$ is the phase speed of the torsional wave in the rod and ρ is the density of the rod. The longitudinal vibration in the rod due to the excitation of a point force $F_0\,e^{j\omega t}$ in the axial direction at $x = x_0$ is also described in the same form as equation (1). For the longitudinal vibration, $\tilde{\theta}(x, t)$ in equation (1) should be replaced by longitudinal displacement $u(x, t)$, c_T by $c_L = \sqrt{E/\rho}$, GI_T by EA (E is Young's modulus and A is the area of cross section) and M_0 by F_0. Therefore the discussion on the convergence properties of the torsional vibration hereafter can be applied to that of the longitudinal vibration as well.

Assuming the torsional rod is fixed at $x = 0$ and a torque is applied to the other end at $x = L$, the corresponding boundary conditions are:

$$\tilde{\theta}(0, t) = 0, \qquad \frac{\partial\tilde{\theta}}{\partial x}(L, t) = \frac{M_0\,e^{j\omega t}}{GI_T}. \tag{2}$$

Using the modal expansion method and mode shape functions of a fixed-free rod, the torsional displacement $\tilde{\theta}(x, t)$ in the rod can be written as follows:

$$\tilde{\theta}(x, t) = \theta(x, \omega)\,e^{j\omega t} = \frac{2M_0}{\rho L I_T}\sum_{m=1}^{\infty}\frac{(-1)^{m+1}\sin\alpha_m x}{\omega_m^2 - \omega^2}\,e^{j\omega t} \tag{3}$$

where

$$\omega_m^2 = \alpha_m^2\frac{G}{\rho}, \qquad \alpha_m = \frac{(2m-1)\pi}{2L}, \qquad m = 1, 2, 3, \ldots . \tag{4}$$

Assuming the angular displacement $\tilde{\theta}(x, t)$ is superimposed by the following two travelling waves:

$$\tilde{\theta}(x, t) = A\,e^{j(\omega t + k_T x)} + B\,e^{j(\omega t - k_T x)}, \tag{5}$$

and using the fixed-free boundary conditions, it can be shown $A = -B = jM_0/(2GI_T k_T \cos k_T L)$ where $k_T = \omega/c_T$. Therefore the angular displacment from the travelling wave method is

$$\tilde{\theta}(x, t) = \frac{M_0 \sin k_T x}{GI_T k_T \cos k_T L}\,e^{j\omega t}. \tag{6}$$

2.2. TORSIONAL ENERGY FLOW

An expression for the time-averaged energy flow carried by the torsional waves in the x direction is:

$$P_T(x) = -\frac{\omega}{2}\,\mathrm{Im}\left\{GI_T\frac{\partial\tilde{\theta}}{\partial x}\,\tilde{\theta}^*\right\} \tag{7}$$

TABLE 1

Parameters used for torsional energy flow

L	5·0 m	ρ	274·0 kg m^{-3}
I_T	$2{\cdot}356 \times 10^{-3}$ m^4	η_T	0·01
G_0	$1{\cdot}0518 \times 10^{10}$ N m^{-2}		

TABLE 2

Parameters used for flexural energy flow

L	1·0 m	ρ	274·0 kg m^{-3}
I_B	$1{\cdot}047 \times 10^{-7}$ m^4	η	0·01
A	$5{\cdot}0 \times 10^{-4}$ m^2	x_0	0·31 m
E_0	$7{\cdot}12 \times 10^{12}$ Nm^{-2}		

where * represents the complex conjugate. Using equation (3) the energy flow by the modal expansion method is

$$P_T(x) = -\frac{2M_0^2\,\omega}{\rho^2 L^2 I_T}\,\mathrm{Im}\left\{G\sum_{m=1}^{\infty}\frac{(-1)^{m+1}\alpha_m\cos\alpha_m x}{\omega_m^2-\omega^2}\sum_{n=1}^{\infty}\frac{(-1)^{n+1}\sin\alpha_n x}{\omega_n^{*2}-\omega^2}\right\} \tag{8}$$

while the travelling wave method gives

$$P_T(x) = -\frac{M_0^2\,\omega}{2I_T}\,\mathrm{Im}\left\{\left(\frac{\cos k_T x}{\cos k_T L}\right)\left(\frac{\sin k_T x}{Gk_T\cos k_T L}\right)\right\}. \tag{9}$$

3. FLEXURAL VIBRATION OF A THIN BEAM

The second example is that of a simply supported beam excited by a harmonic point force $F_0\,e^{j\omega t}$ at $x = x_0$. Although the solution of the beam flexural response by either the

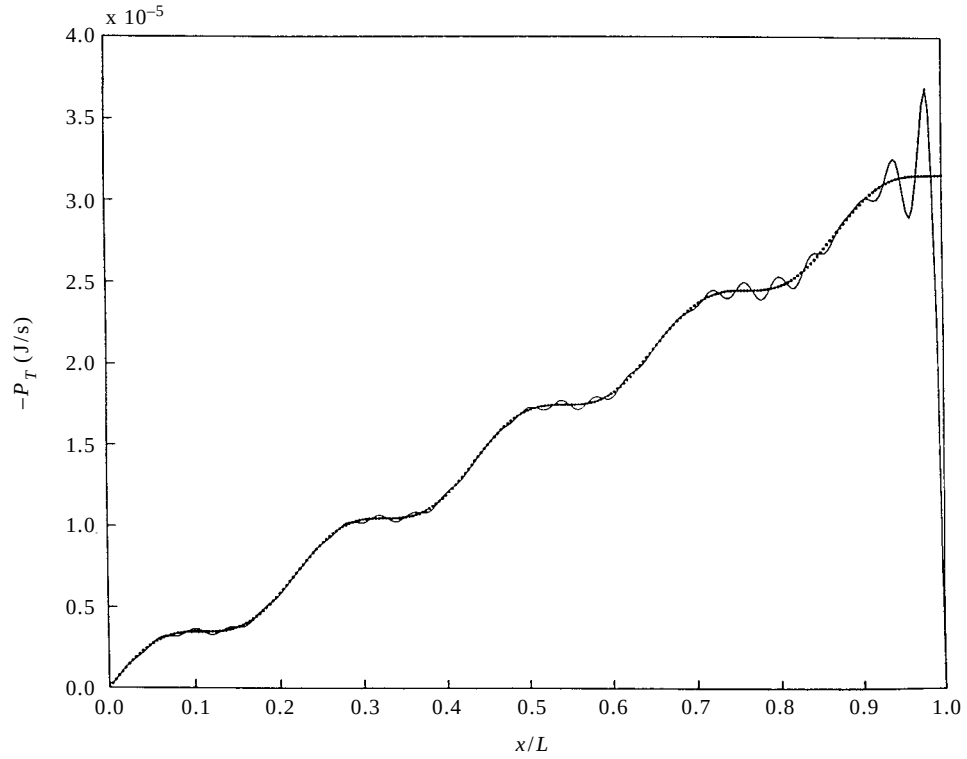

Figure 1. Torsional energy flow P_T at 900 Hz. Solid curve: by MEM (50 modes), dotted curve: by TWM.

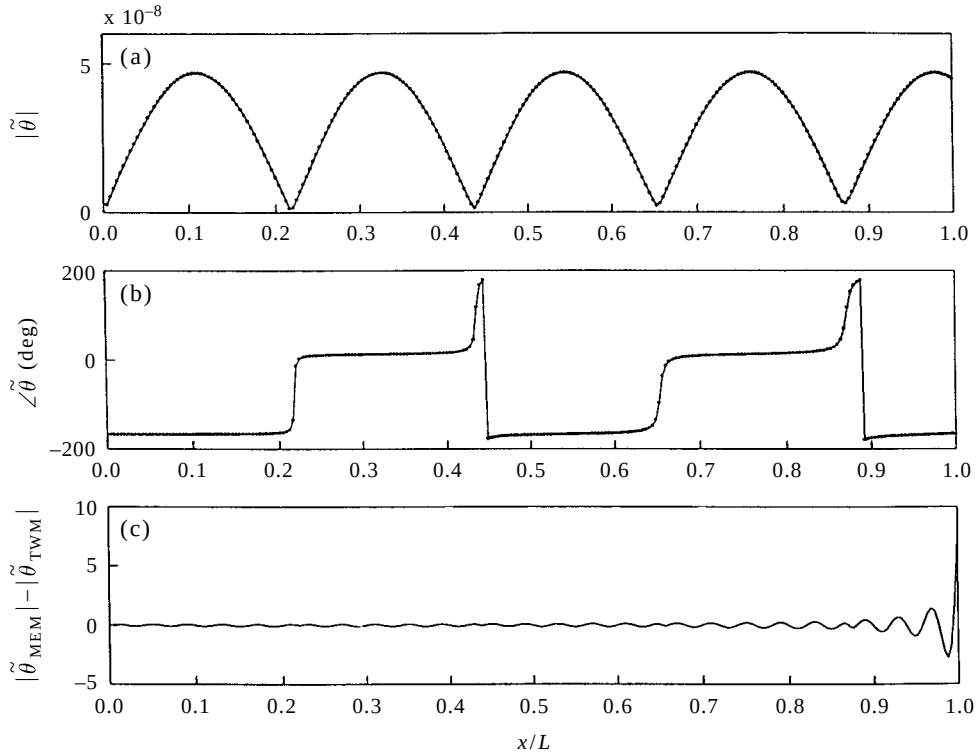

Figure 2. Angular displacement of the rod at 900 Hz. (a) Magnitudes of $\tilde{\theta}$, (b) phases of $\tilde{\theta}$ [solid curve: by MEM (50 modes), dotted curve: by TWM], and (c) $|\tilde{\theta}|_{\mathrm{MEM}} - |\tilde{\theta}|_{\mathrm{TWM}}$.

modal expansion method or the travelling wave method is a trivial exercise, the comparison of the energy flow by the two methods, however, may give some insight into the convergence property of the predicted energy flow carried by flexural waves.

3.1. FORCED RESPONSE OF THE BEAM FROM MEM AND TWM

According to the modal expansion method, the displacement reponse, $W(x)\,\mathrm{e}^{j\omega t}$, can be expressed as:

$$W(x) = \frac{2F_0}{\rho LA} \sum_{m=1}^{\infty} \frac{\sin \beta_m x_0 \sin \beta_m x}{\omega_m^2 - \omega^2} \tag{10}$$

where

$$\beta_m = \frac{m\pi}{L}, \qquad \omega_m = \beta_m^2 \sqrt{\frac{EI_B}{\rho A}}, \qquad m = 1, 2, 3, \ldots \tag{11}$$

and E, ρ, I_B, L, A are respectively the complex Young's modulus [$E = E_0(1 + j\eta)$, η is the tensile loss factor], density, moment about the neutral plane, length and area of the cross section of the beam.

On the other hand, the travelling wave solution of the one-dimensional bending wave equation gives the following general solution:

$$W(x) = \begin{cases} W_1(x) = A_1 e^{kx} + A_2 e^{-kx} + A_3 e^{jkx} + A_4 e^{-jkx}, & (x \leqslant x_0) \\ W_2(x) = A_5 e^{kx} + A_6 e^{-kx} + A_7 e^{jkx} + A_8 e^{-jkx}, & (x \geqslant x_0) \end{cases} \tag{12}$$

where $k^2 = \sqrt{(\rho A/EI_B)}$ and the coefficients $A_1, A_2, \ldots, A_8$ are determined by the boundary conditions at $x = 0$, $x = L$ (in this analysis simply supported boundary conditions are assumed) and the joint conditions at $x = x_0$. The solution of the coefficients can be obtained as illustrated in Appendix A.

3.2. FLEXURAL ENERGY FLOW

The energy flow carried by flexural waves through a cross section of the beam can be expressed as:

$$P_B(x) = \frac{\omega}{2} \operatorname{Im}\left\{EI_B\left(\frac{\partial W^*}{\partial x}\frac{\partial^2 W}{\partial x^2} - W^*\frac{\partial^3 W}{\partial x^3}\right)\right\} \tag{13}$$

where EI_B is the bending rigidity of the beam.

4. RESULTS AND DISCUSSION

In this section, the torsional and flexural energy flows in two beam structures are calculated using the modal expansion method and travelling wave method. Table 1 lists the parameters of a rod with fixed-free boundary conditions for the torsional energy flow. The parameters of a thin beam with simply supported boundary conditions for the flexural

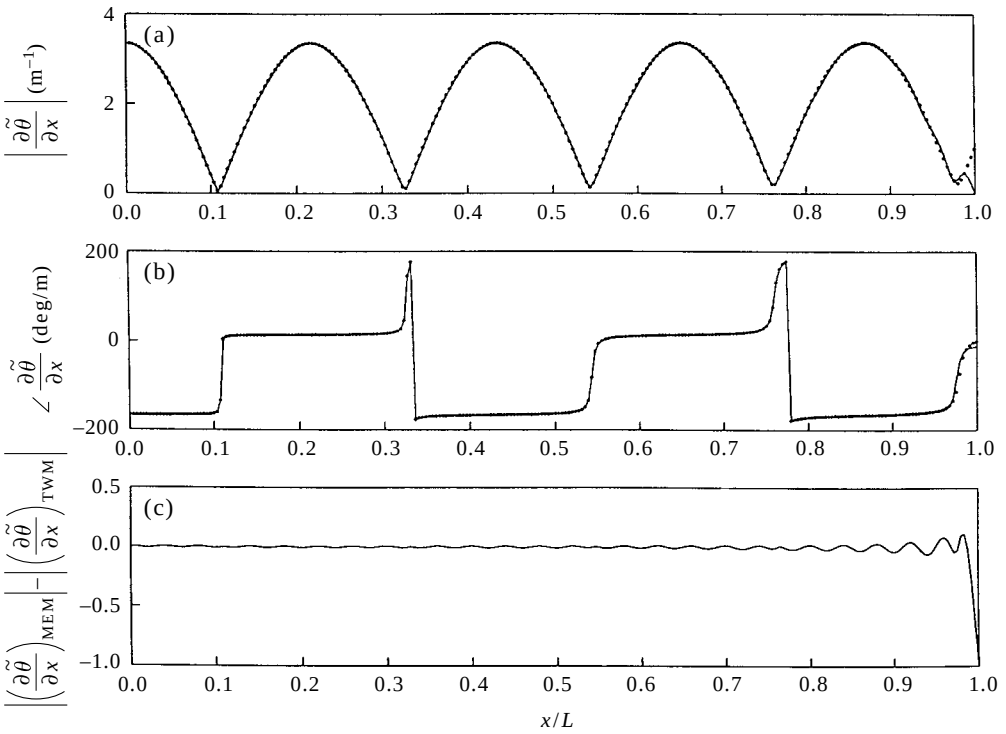

Figure 3. Derivative of angular displacement of the rod at 900 Hz. (a) Magnitudes of $\partial\theta/\partial x$, (b) phases of $\partial\tilde{\theta}/\partial x$ [solid curve: by MEM (50 modes), dotted curve: by TWM] and (c) $|\partial\tilde{\theta}/\partial x|_{\mathrm{MEM}} - |\partial\tilde{\theta}/\partial x|_{\mathrm{TWM}}$.

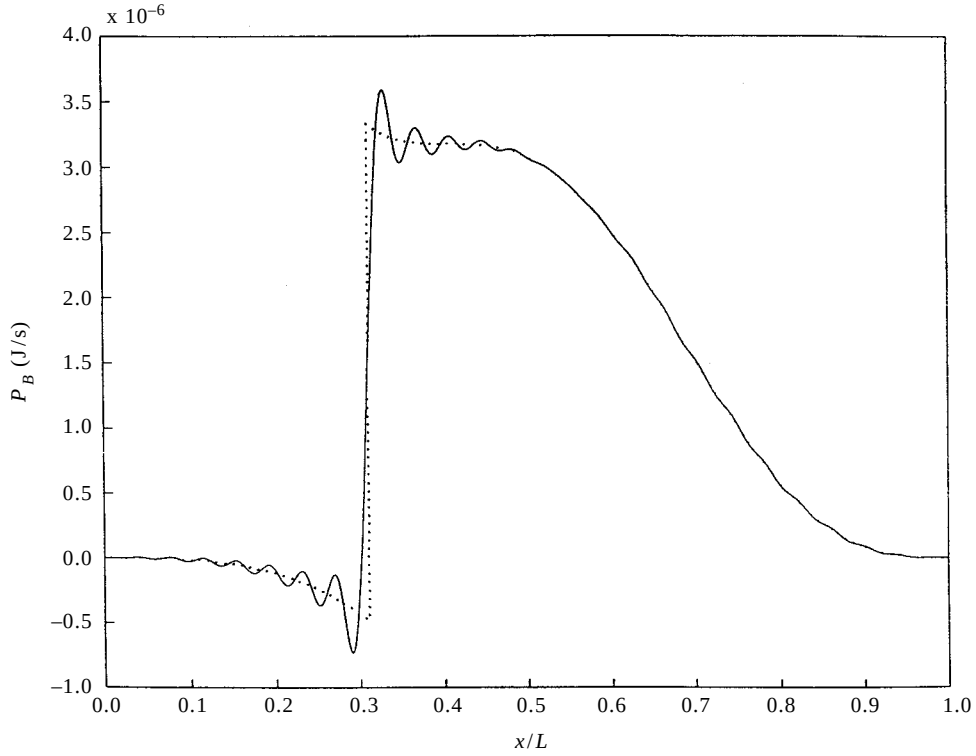

Figure 4. Flexural energy flow P_B at 270 Hz. Solid curve: by MEM (50 modes), dotted curve: by TWM.

energy flow are shown in Table 2. The energy flow in each structure is predicted using MEM and TWM. Results are compared and the sources of the energy flow fluctuation when MEM is used about the exact energy flow are analysed in terms of the convergence properties of the modal expansion series for the displacement response and its derivatives. Although the modal truncation error causes an inaccurate prediction of the energy flow, the spatial-averaged energy flow appears to give a good approximation to the exact value. Finally, the prediction of energy flow due to the driving force and moment is considered. The input energy flow can be predicted accurately using the modal expansion method when the input forcing function is used directly instead of that calculated from the constitutive relationships.

Figure 1 shows the torsional energy flow in a rod excited by a unit torque at $x = L$. The frequency of excitation is 900 Hz. The solid curve was obtained using MEM with 50 modes while the dotted one was calculated using TWM. The fluctuation of the energy flow from MEM decreases at observation point away from the driving torque.

To study the source of the fluctuation of the predicted energy flow, the torsional displacement $\tilde{\theta}$ and its derivative $\partial\tilde{\theta}/\partial x$ by MEM and TWM are shown in Figures 2 and 3 respectively. The differences between $\tilde{\theta}$ and its derivative $\partial\tilde{\theta}/\partial x$ for the two methods are also shown in the figures. It can be seen that the difference in magnitude and phase of the angular displacements predicted by the two methods are very small. The maximum difference of the angular displacement is smaller than the magnitude of the angular displacement itself by an order of two. This indicates that 50 modes used in the modal expansion method are sufficient for the prediction of the torsional displacement response for this case. However, significant differences [as shown in Figure 3(a)] are found in the

derivatives of the angular displacement $\partial\tilde{\theta}/\partial x$ (related to the torsional stress), particularly at the cross sections near the driving torque. For this case the difference of the derivatives by the two methods is nearly of the same order as the derivatives themselves. The convergence of the displacement from the modal expansion method can be approximately described by the series $\Sigma_N^\infty\ 1/n^2$, where N is the mode number whose resonance frequency is first larger than the driving frequency [7]. However, the convergence of the derivative of the displacement is approximated by $\Sigma_N^\infty\ 1/n$. Clearly, a given number of modes may give a sufficient accuracy in the predicted displacement response, but may not give the same level of accuracy in the predicted derivatives of the response.

At the driving frequency, the contribution of the errors in the displacement and its derivative to the error in the energy flow by MEM can be explained as in the following analysis. Using the modal expansion method, the exact displacement $\overline{\theta}$ can be expressed by the sum of the approximate displacement $\overline{\theta}$ due to the expansion of a finite number of modes and displacement error $\Delta\overline{\theta}$:

$$\tilde{\theta} = \overline{\theta} + \Delta\overline{\theta}. \tag{14}$$

Similarly, the exact derivative of the displacement can be expressed as:

$$\tilde{\theta}' = \overline{\theta}' + \Delta\overline{\theta}'. \tag{15}$$

From equations (7), (14) and (15), the error in the energy flow due to the use of finite number of modes is:

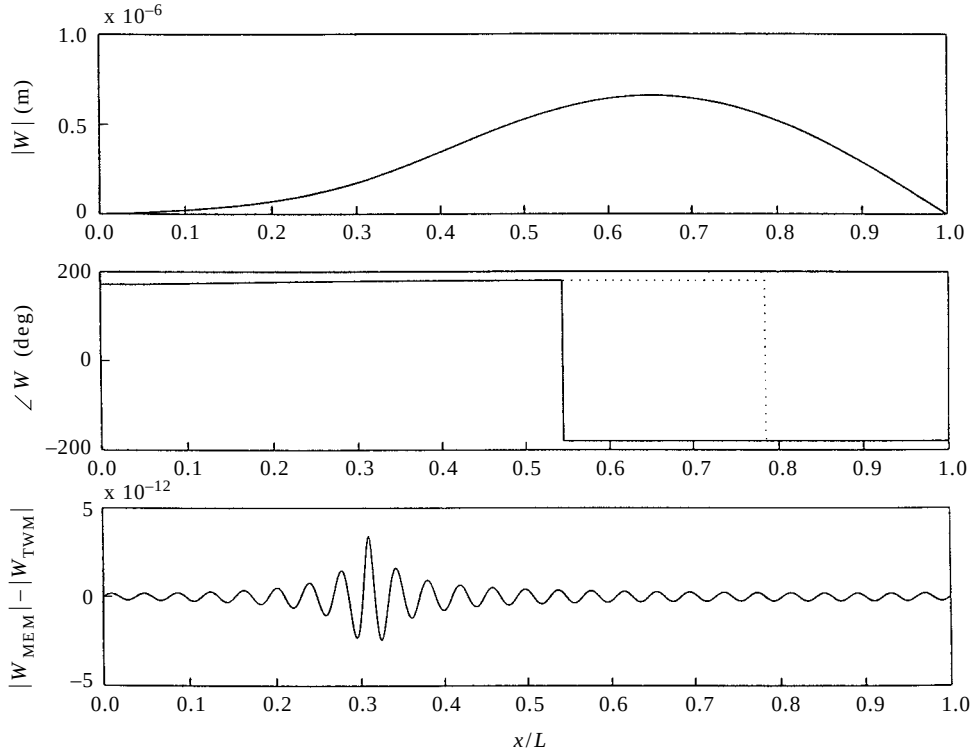

Figure 5. Displacement W of the beam at 270 Hz. (a) Magnitudes of W, (b) phases of W [solid curve: by MEM (50 modes), dotted curve: by TWM] and (c) $|W|_{\mathrm{MEM}} - |W|_{\mathrm{TWM}}$.

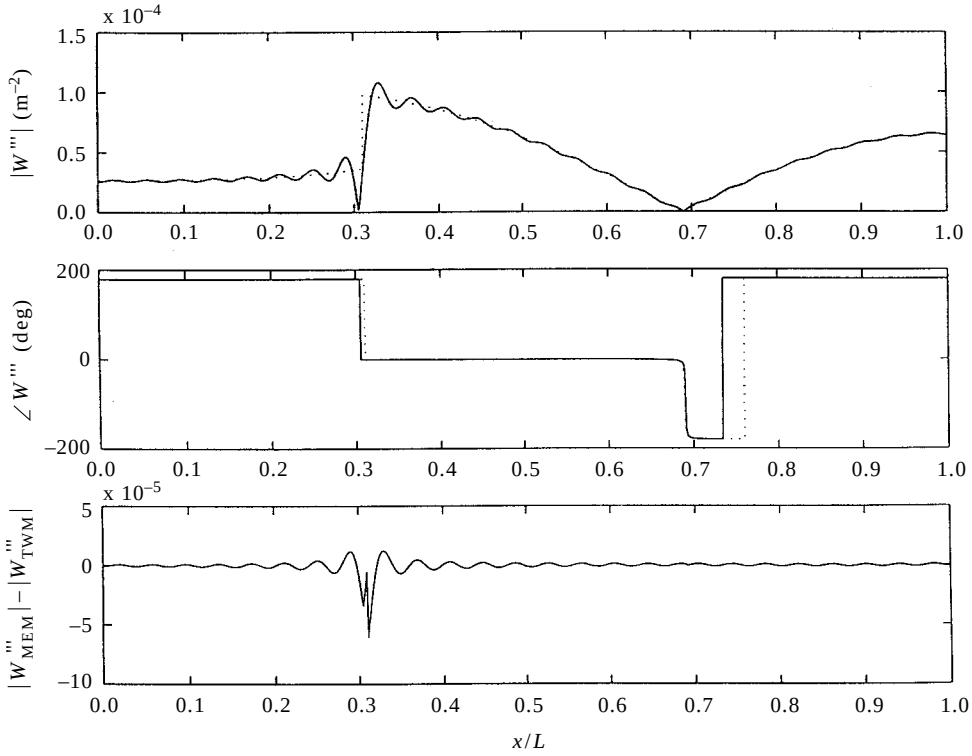

Figure 6. Third derivative W''' of displacement of the beam at 270 Hz. (a) Magnitudes of W''', (b) phases of W''' [solid curve: by MEM (50 modes), dotted curve: by TWM] and (c) $|W'''|_{\mathrm{MEM}} - |W'''|_{\mathrm{TWM}}$.

$$\Delta P_T(x) = -\frac{\omega}{2}\,\mathrm{Im}\,\{GI_T(\Delta\overline{\theta}'\overline{\theta}^* + \overline{\theta}'\overline{\theta}^* + \Delta\overline{\theta}'\Delta\overline{\theta}^*)\}. \tag{16}$$

Using the magnitudes of $\overline{\theta}$, $\Delta\overline{\theta}$, $\overline{\theta}'$ and $\Delta\overline{\theta}$ shown in Figures 2 and 3, the terms which are responsible for the fluctuation in $\Delta P_T(x)$ can be identified. Away from the excitation location, Figures 2 and 3 show that the error terms $\Delta\overline{\theta}$ and $\Delta\overline{\theta}'$ have magnitude of the order of 10^{-10} and 10^{-1} respectively. However, the maximum values for $\overline{\theta}$ and $\overline{\theta}$ are approximately $4{\cdot}8 \times 10^{-8}$ and $3{\cdot}4$ respectively. It can therefore be seen that both $\Delta\overline{\theta}$ and $\Delta\overline{\theta}'$ may have significant contribution to the error in the energy flow. This is because the error in the energy flow depends on the cross products $\Delta\overline{\theta}'\theta^*$ and $\overline{\theta}'\Delta\theta^*$. Although $\Delta\overline{\theta}$ is relatively small, it is amplified by a large value of $\overline{\theta}'$. On the other hand, the large $\Delta\overline{\theta}'$ is multiplied by a small displacement $\overline{\theta}$. As a result, the two products have comparable magnitudes.

Figure 4 shows the flexural energy flow in a simply supported beam at 270 Hz. A point force of unit amplitude is applied at $x = 0{\cdot}31$ m of the beam. The fluctuation of predicted flexural energy flow by MEM using 50 modes is also observed in the vicinity of the driving force. The source of the fluctuation can also be traced in terms of the convergence properties of the flexural response and its higher order derivatives. For the prediction of flexural energy flow, the calculation of the second and third order derivatives of the beam displacement is required for the bending moment and shear force in the beam. The convergence property of the flexural displacment is described by $\Sigma_N^\infty\, 1/n^4$, while that of the shear force and bending moment are approximated by $\Sigma_N^\infty\, 1/n$ and $\Sigma_N^\infty\, 1/n^2$ respectively. As a result, it is expected that the shear force will suffer the largest modal truncation error.

Figure 6 shows the third derivative of the response. The discontinuity of the shear force is clearly identified in the vicinity of the driving force. The superposition of a finite number of continuous modes is insufficient to represent such a force discontinuity. Therefore, a large error is introduced. The contribution of the errors in predicting the response and its derivatives to the error in the flexural energy flow due to the use of a finite number of modes can also be analysed in a similar way to that of the torsional energy flow. Using $\bar{W}$, $\bar{W}'$, $\bar{W}''$ and $\bar{W}'''$ for the approximate beam displacement and its derivatives due to a finite expansion of modes, $\Delta\bar{W}$, $\Delta\bar{W}'$, $\Delta\bar{W}''$ and $\Delta\bar{W}'''$ for the corresponding error terms, the error in the flexural energy flow can be expressed as:

$$\Delta P_B(x) = \frac{\omega}{2}\,\mathrm{Im}\,\{EI_B\,[(\Delta\bar{W}')^*\bar{W}'' + (\bar{W}')^*\Delta\bar{W}'' + (\bar{W})^*\Delta\bar{W}'''' + (\Delta\bar{W})^*\bar{W}'''' + (\Delta\bar{W}')^*\Delta\bar{W}'' + (\Delta\bar{W})^*\Delta\bar{W}'''']\}. \tag{17}$$

A similar analysis to that used for the torsional energy flow can be used to evualate the main sources of the error in the predicted energy flow. It is obvious that error in the energy flow is not only dependent upon the errors in the displacement and its derivatives, but also on the magnitudes of the approximate displacement and its derivatives. Figure 5 shows the distributed displacement response (magnitude $|W|$ and phase $\langle W$) of the flexural beam at a frequency of 270 Hz. Figure 6 shows the distributed higher order derivative $\bar{W}''''$ and $\Delta\bar{W}''''$. They are used to evaluate some of the products in equation (17) and explain the cause of the error in predicting the distributed energy flow by MEM in Figure 4. It has been shown that the largest flucuation in energy flow from MEM occurs at the driving location because the discontinuity of the internal stress there is difficult to represent by continuous mode shape functions. It is also shown that the structural response predicted by MEM is sufficiently accurate without using a large number of modes. One would expect to have a large error in the predicted input power at the driving location when the forcing term is calculated by $EI_B W''''$. For this case the external force must be used instead in order to give an accurate prediction of input power [7].

An interesting observation of the fluctuation in the predicted energy flow using MEM is its oscillating nature. The magnitude of the oscillation increases as the observation location approaches the driving location. Further investigation reveals two other features in the energy flow predicted using MEM:

(1) At any cross-section, the absolute deviation of the predicted energy flow by MEM from the exact one reaches its maximum as the driving frequency coincides with one of the resonance frequencies of the beam. Figure 7(a) shows the deviations of torsional energy flow evaluated at four cross-sections corresponding to $x = 0{\cdot}3,\ 0{\cdot}7,\ 0{\cdot}95,\ 0{\cdot}98\,L$ as functions of the driving frequency (for this case $x = 0{\cdot}31\,L$ corresponds to the source location). The peaks in all the deviation curves correspond exactly to the torsional resonance frequencies of the rod at 98·0, 293·9, 489·8, 685·7, 881·7 Hz. The reason for the maximum error in torsional energy flow occurring at the resonance frequencies can be readily explained using equation (16). Although the error in the response and torsional stress due to a finite modal expansion remains of the same order at both resonance and non-resonance frequencies, the error in the energy is contributed by the product terms $\Delta\bar{\theta}'\bar{\theta}^*$ and $\bar{\theta}'\Delta\bar{\theta}^*$. Near the resonance frequencies, the approximate angular displacement and its derivative reach a maximum. They are attributed to the large values in the product terms and the large error in the predicted energy flow. Similar results were observed in the absolute energy flow deviation of flexural waves in the beam as a function of frequency [see Figure 7(b)]. The peak deviations at the resonance frequencies of the beam (115·9,

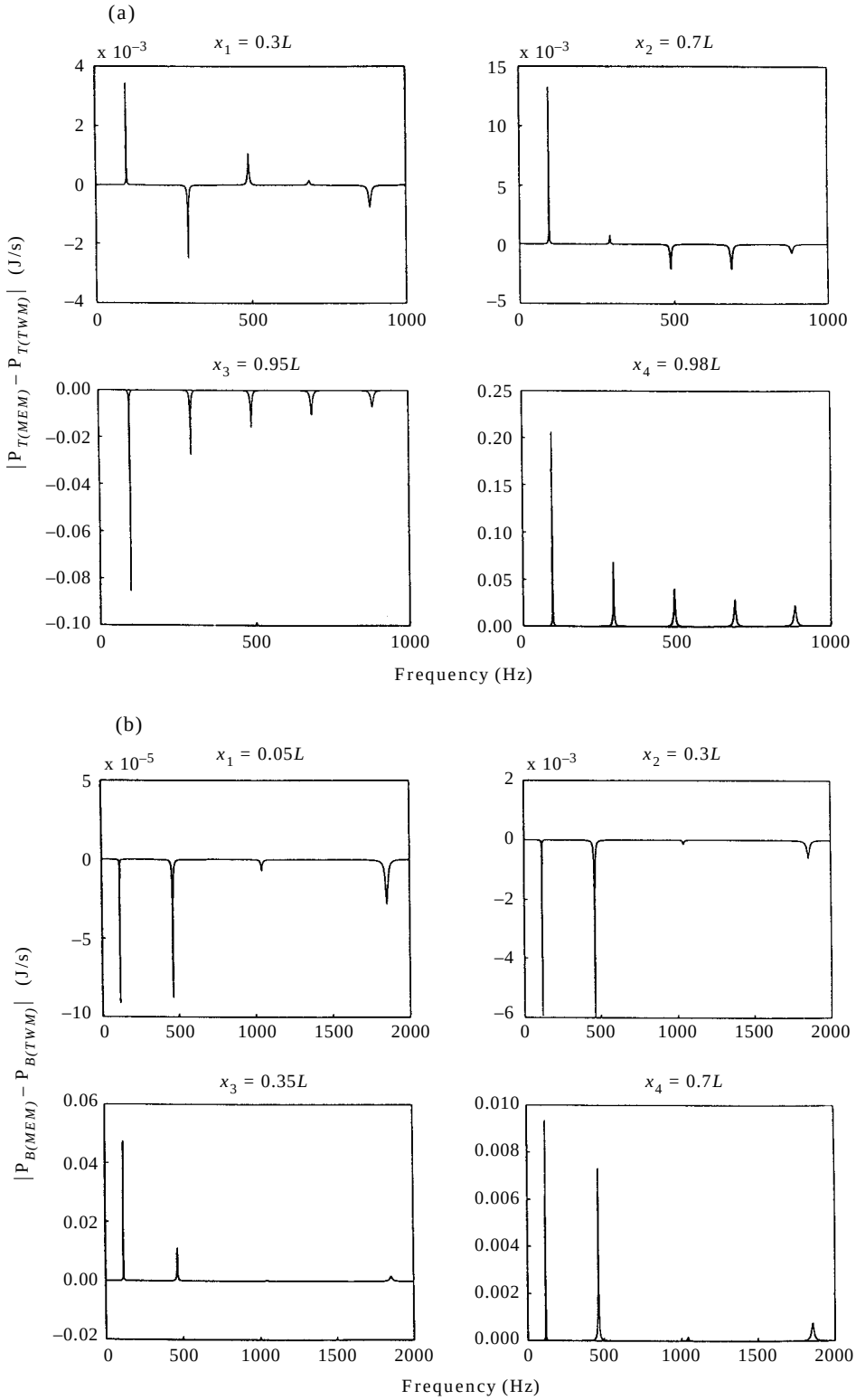

Figure 7. Difference of energy flow by MEM and TWM as function of frequency. (a) For torsional energy flow in the rod and (b) for flexural energy flow in the beam.

463·5, 1042·8 and 1853·9 Hz can also be explained by the contribution of the large response and its derivatives to the product terms in equation (17).

(2) It is observed that in the near field of the driving source the average fluctuation period of the distributed deviation in energy flow is independent of the vibrational frequency as long as the total number of modes M used in the modal expansion is unchanged. Increasing M, however, will reduce the average spatial fluctuation period. Figures 8 and 9 show the absolute deviations of torsional and flexural energy flow in the near-field areas of the beam structures. Three values of M are used for the observations of the relationship between the spatial period and M. Each subplot in the figures corresponds to a constant M. The solid, dotted and dashed curves correspond to different driving frequencies given in the figure captions. It can be seen that all the curves in each subplot intersect with the x axis at the same locations. This indicates that the spatial fluctuation of energy flow by MEM is a function of M. The observation of the fluctuation in torsional and flexural energy flow shows that the average spatial period seems to be approximately equal to the wavelength of the lowest [the $(M + 1)$th order] mode being truncated. For the torsional energy flow the spatial period of fluctuation is $\lambda^{(T)}_{M+1} = 2L/M$, and for the flexural energy flow the period is $\lambda^{(B)}_{M+1} = 2L/(M + 1)$. It should be noted that the energy flow deviation in each spatial cycle includes positive values in half cycle and negative in the other. Obviously, a spatial average of the energy flow from the MEM within each cycle may give rise to a better representation of the energy flow near the driving force location. However, the determination of an optimal spatial average approach (e.g. determination of the weighting function in the weighted spatial average algorithm) for obtaining the energy flow

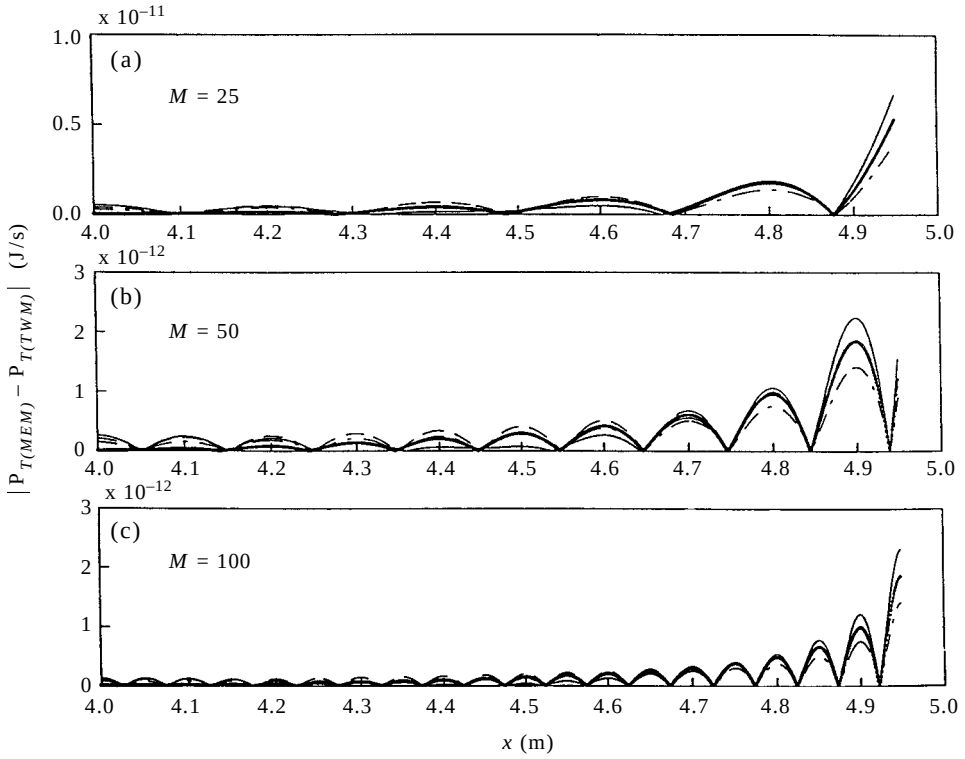

Figure 8. Absolute deviation of the predicted torsional energy flow by MEM from that by TWM. The solid, dotted, dashed and dashed- dotted curves correspond respectively to the driving frequencies at 900, 500, 100 and 50 Hz.

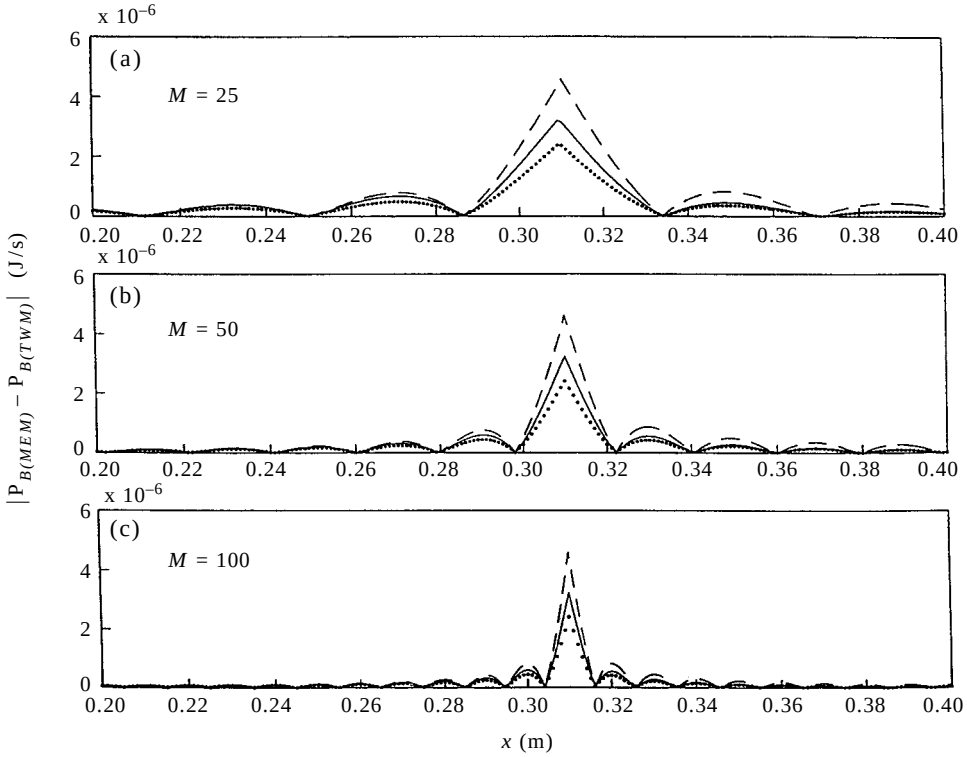

Figure 9. Absolute deviation of the predicted flexural energy flow by MEM from that by TWM. The solid, dotted and dashed lines correspond respectively to the driving frequencies at 600, 300 and 100 Hz.

with minimum influence of modal truncation error remains the task of further investigation.

As the mode shape functions satisfy the selected boundary conditions used in this paper, the effect of the modal truncation on energy flow at near field of the boundaries becomes unimportant. However, if the mode shape functions do not satisfy the boundary conditions, such as for the case of sound field with complex acoustical admittance as its boundaries [7], this effect will become significant.

5. CONCLUSIONS

The energy flow predicted by the modal expansion method may suffer from slow convergence problems and modal truncation error in the area near the driving location. The sources of the truncation errors in the predicted energy flow essentially come from the error in the estimation of the beam response and its derivatives, and from the difficulty to represent the force discontinuity at the driving location using a limited number of continuous mode shape functions. The investigation of the fluctuation of the predicted energy flow by MEM shows that spatial averaged energy flow can give more accurate approximation of the energy flow when a limited number of modes only are used in the modal expansion and modal truncation error is significant.

It is also shown that the input force must be used directly for the calculation of energy flow at the input location because the largest modal truncation error in the calculation of internal stresses using the constitutive relationship occurs at the driving location.

ACKNOWLEDGMENT

Financial support for this work from Australia Research Council is gratefully acknowledged.

REFERENCES

1. L. Meirovitch 1967 *Analytical Methods in Vibration*. New York: Macmillan.
2. L. D. Pope and J. F. Willy 1977 *Journal of the Acoustical Society of America* **62**, 906–911. Band-limited power flow into enclosures.
3. K. Sum and J. Pan 1996 submitted *Journal of the Acoustical Society of America*. An analytical model for band-limited response of acoustic-structural coupled systems, Part I: mathematical development.
4. R. L. Clark Jr, C. R. Fuller and A. Wicks 1991 *Journal of the Acoustical Society of America* **90**, 346–357. Characterisation of multiple piezoelectric actuators for structural excitation.
5. R. L. Clark 1996 *Journal of the Acoustical Society of America* **99**, 627–630. Approximating the response of reverberant systems: applications to proportional damping, added impedance, and feedback control.
6. T. E. Rook and R. Singh 1996 *Journal of the Acoustical Society of America* **99**, Pt. 1, 2158–2166. Modal truncation issues in synthesis procedures for vibratory power flow and dissipation.
7. J. Pan 1995 *Journal of the Acoustical Society of America* **97**, 691–694. A second note on acoustic intensity.

APPENDIX A: THE TRAVELLING WAVE COEFFICIENTS OF SIMPLY SUPPORTED BEAM

Substituting the travelling wave solution, equation (13), into the following four boundary conditions:

$$W_1|_{x=0} = 0, \qquad \left.\frac{\partial^2 W_1}{\partial x^2}\right|_{x=0} = 0, \qquad W_2|_{x=L} = 0, \qquad \left.\frac{\partial^2 W_2}{\partial x^2}\right|_{x=L} = 0, \tag{A1}$$

and four joint conditions:

$$W_1|_{x=x_0} = W_2|_{x=x_0}, \qquad \left.\frac{\partial W_1}{\partial x}\right|_{x=x_0} = \left.\frac{\partial W_2}{\partial_x}\right|_{x=x_0}, \qquad \left.\frac{\partial^2 W_1}{\partial x^2}\right|_{x=x_0} = \left.\frac{\partial^2 W_2}{\partial x^2}\right|_{x=x_0}, \tag{A2a}$$

$$\left.\frac{\partial^3 W_2}{\partial x^3}\right|_{x=x_0} - \left.\frac{\partial^3 W_1}{\partial x^3}\right|_{x=x_0} = \frac{F_0}{EI}, \tag{A2b}$$

a set of linear equations can be obtained. The coefficients $A_1, \ldots, A_8$ in equation (13) are calculated from the solution of the following matrix equation:

$$\Phi A = B \tag{A3}$$

where

$$A = (A_1, A_2, A_3, A_4, A_5, A_6, A_7, A_8)^T \tag{A4}$$

$$B = \left(0, 0, 0, 0, 0, 0, 0, \frac{F_0}{EIk^3}\right)^T \tag{A5}$$

and

$$\Phi = \begin{bmatrix} 1 & 1 & 1 & 1 & 0 & 0 & 0 & 0 \\ 1 & 1 & -1 & -1 & 0 & 0 & 0 & 0 \\ 0 & 0 & 0 & 0 & e^{kL} & e^{-kL} & e^{jkL} & e^{-jkL} \\ 0 & 0 & 0 & 0 & e^{kL} & e^{-kL} & -e^{jkL} & -e^{-jkL} \\ e^{kx_0} & e^{-kx_0} & e^{jkx_0} & e^{-jkx_0} & -e^{kx_0} & -e^{-kx_0} & -e^{jkx_0} & -e^{-jkx_0} \\ e^{-kx_0} & -e^{-kx_0} & je^{jkx_0} & -je^{-jkx_0} & -e^{-kx_0} & e^{-kx_0} & -je^{jkx_0} & je^{-jkx_0} \\ e^{-kx_0} & e^{-kx_0} & -e^{jkx_0} & -e^{-jkx_0} & -e^{kx_0} & -e^{-kx_0} & e^{jkx_0} & e^{-jkx_0} \\ -e^{-kx_0} & e^{-kx_0} & je^{jkx_0} & -je^{-jkx_0} & e^{-kx_0} & -e^{-kx_0} & -je^{jkx_0} & je^{-jkx_0} \end{bmatrix}. \tag{A6}$$